The EMBO Journal vol.11 no.7 pp.2373-2379, 1992

Three-dimensional structure of transketolase, a thiamine diphosphate dependent enzyme, at 2.5 Å resolution

Ylva Lindqvist[2], Gunter Schneider[2], Ulrich Ermler[1] and Michael Sundström

Department of Molecular Biology, Swedish University of Agricultural Sciences, Uppsala Biomedical Center, Box 590, S-75124 Uppsala, Sweden
[1]Present address: Max-Planck-Institut für Biophysik, Heinrich-Hoffmann-Strasse 7, 6000 Frankfurt 71, Germany
[2]Corresponding authors

Communicated by C.I.Brändén

The crystal structure of *Saccharomyces cerevisiae* transketolase, a thiamine diphosphate dependent enzyme, has been determined to 2.5 Å resolution. The enzyme is a dimer with the active sites located at the interface between the two identical subunits. The cofactor, vitamin B_1 derived thiamine diphosphate, is bound at the interface between the two subunits. The enzyme subunit is built up of three domains of the α/β type. The diphosphate moiety of thiamine diphosphate is bound to the enzyme at the carboxyl end of the parallel β-sheet of the N-terminal domain and interacts with the protein through a Ca^{2+} ion. The thiazolium ring interacts with residues from both subunits, whereas the pyrimidine ring is buried in a hydrophobic pocket of the enzyme, formed by the loops at the carboxyl end of the β-sheet in the middle domain in the second subunit. The structure analysis identifies amino acids critical for cofactor binding and provides mechanistic insights into thiamine catalysis.
Key words: protein crystallography/thiamine diphosphate/transketolase

Introduction

Transketolase is a key enzyme in the pentose phosphate pathway for the metabolism of glucose-6-phosphate. The enzyme catalyses ketol transfer from a ketose to an aldose amongst a variety of donor and acceptor sugar phosphates. Transketolase, together with transaldolase, creates a reversible link between two main metabolic pathways, the pentose phosphate pathway and glycolysis. This allows the cell to adapt to a variety of needs such as production of NADPH (reducing power) for biosynthesis, ribose-5-phosphate for synthesis of DNA or supply of glycolytic intermediates. In photosynthetic organisms, the enzyme is also part of the Calvin cycle, where ribulose-1,5-bisphosphate is regenerated from phosphoglycerate formed during fixation of CO_2.

Transketolase from baker's yeast, *Saccharomyces cerevisiae*, is composed of two identical subunits (Cavalieri *et al.*, 1975) each with a molecular weight of 74 000 (Sundström *et al.*, unpublished results). The enzyme contains thiamine diphosphate (ThDP, scheme 1), the biologically active derivative of vitamin B_1 as a prosthetic group and requires Mg^{2+} ions for catalytic activity. Other metal ions such as Ca^{2+}, Mn^{2+} and Co^{2+} can replace the Mg^{2+} ion (Heinrich *et al.*, 1972). The amino acid sequences derived from the DNA sequences for transketolase from *Rhodobacter sphaeroides* (Chen *et al.*, 1991), *S.cerevisiae* (M.Sundström, Y.Lindqvist, U.Hellman, G.Schneider and H.Ronne, unpublished results) and a formaldehyde transketolase from the yeast *Hansenula polymorpha* (Janowicz *et al.*, 1985) have been determined.

ThDP serves as cofactor in many biochemical reactions involving cleavage of the carbon–carbon bond adjacent to a keto-group. Important members of this class of ThDP dependent enzymes are pyruvate decarboxylase, transketolase and the 2-oxo acid decarboxylase component of the 2-oxo acid dehydrogenase complex. Whereas non-enzymatic catalysis by thiamine has been rather well studied (for a review see Kluger, 1987), enzyme mediated thiamine catalysis is poorly understood, mainly due to the lack of structural information on enzyme–cofactor and enzyme–cofactor–substrate interactions. In the following, we describe the molecular structure of a ThDP dependent enzyme at high resolution and its interactions with the bound cofactor, and discuss implications for enzymatic thiamine catalysis.

Results

Electron density map

The electron density map at 2.9 Å resolution calculated with phases from multiple isomorphous replacement (mean figure of merit 0.54) was not interpretable. This map could be improved, however, by non-crystallographic averaging (Bricogne, 1976) using local twofold symmetry. The averaged map allowed us to build a partial polyalanine model of the protein, consisting of 355 amino acids per subunit. A cyclic bootstrapping procedure of phase combination of model phases with multiple isomorphous replacement phases followed by model building and refinement improved the electron density gradually such that the polypeptide chain could be traced. The current model consists of residues 3–680, one Ca^{2+} ion and one cofactor molecule per subunit and has a crystallographic R-factor of 0.215 at 2.5 Å resolution and r.m.s. bond length deviation of 0.024 Å. Figure 1 shows the electron density for bound ThDP at the active site of transketolase.

Overall structure

Transketolase is a dimeric molecule where the twofold related active sites are located between different domains

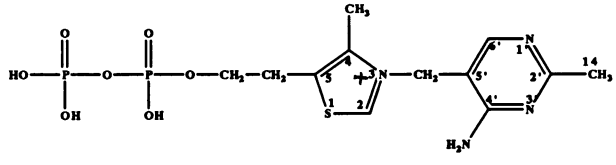

Scheme 1. Nomenclature used for thiamine diphosphate.

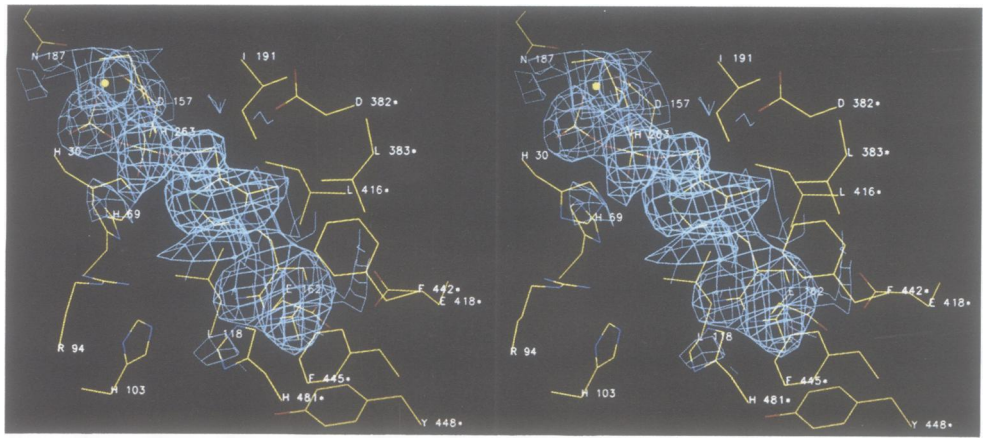

Fig. 1. Stereo view of the final $2|F_o| - |F_c|$ electron density map of holo-transketolase at the location of bound thiamine diphosphate. The contour level of the electron density is at the standard deviation of the electron density map. The refined structure of the active site is superimposed.

of the two subunits. Residues from both subunits build up the active site and are involved in binding the cofactor. Therefore, the dimer is the functional unit of transketolase. This arrangement of the coenzyme binding site gives a molecular explanation for the observation that the addition of ThDP prevents the dissociation of apo-transketolase into monomers at low protein concentrations (Cavalieri *et al.*, 1975). Also, it is compatible with the observed co-operativity of the apoenzyme with regard to cofactor binding (Egan and Sable, 1981).

The subunit. The 680 amino acids of the V-shaped subunit are folded into three consecutive α/β-domains (Figure 2). The N-terminal domain (residues 3–322) consists of a five-stranded parallel β-sheet with topology $+1X, +1X, +2X, -1X$. There are several helices on both sides of the sheet and some additional helices not belonging to this structural motif on top of it. In the β/α connection after the second strand in the β-sheet there is an extra helix and the β/α connection after the third strand contains a hairpin loop. Both of these loops are involved in cofactor binding. The chain leaves this domain via a long helix of 33 residues which contains one turn of π-helix after one third of its length.

The second domain (residues 323–538) contains a parallel β-sheet of six strands with topology $-1X, +2X, +1X, +2X, -1X$. The structural motif of the second domain is very similar to the first domain, especially in the last four α/β-units of the domains. Alignment of the Cα carbon atoms of the two domains using the program O (Jones *et al.*, 1991) gave an r.m.s. fit of 2.2 Å for 120 atoms from all five α/β-units which were structurally equivalent in the two domains.

This comparison reflects more similarity than could be expected from any two parallel sheets with the same topology as inferred from comparison of the second domain to a parallel sheet in glucose-6-phosphate isomerase which has exactly the same topology (Shaw and Muirhead, 1977). That comparison gave an r.m.s. deviation of 2.3 Å but only 55 atoms were structurally equivalent. It is thus probable that domains one and two of transketolase are evolutionary related although the structurally equivalent 120 residues share only 13% identical amino acids.

Loops at the carboxyl end of the β-sheet in the second domain are also involved in binding ThDP and probably in binding the substrates.

Finally, the third domain (residues 539–680) consists of a β-sheet with one antiparallel strand followed by four parallel strands with the ubiquitous topology shown in Figure 2b. The cleft formed between strands 19 and 21 created by a crossover connection (Brändén, 1980) is far away from the active sites. It seems to be filled up by rather large side chains but it could form a binding site for regulatory molecules.

The dimer. A schematic view of the transketolase dimer is shown in Figure 3. The interface region of the dimer consists of a buried surface of 4390 Å^2. There are tight packing interactions between helices 8 and 9 on one side of the sheet in the N-terminal domain with the twofold related helices in the other subunit (Figure 3b). The surface area buried in the N-terminal domain upon dimer formation is 1550 Å^2. The interaction between the subunits in the C-terminal domain mainly involves contacts between the C-termini (Figure 3a). The buried surface for this domain corresponds to an area of 1170 Å^2. The main contacts between the middle domains involve the twofold related helices 19. This dimer arrangement positions the loops at the carboxy end of the sheet of the N-terminal domain of one subunit in contact with the loops at the carboxy end of the middle domain of the second subunit. Most of these interactions are in or close to the active site.

The two subunits were built and refined independently with no restraints included for the non-crystallographic symmetry. The subunits obey the local twofold symmetry axis very closely. Superposition of one subunit with the other gives an r.m.s. deviation of 0.35 Å for all 678 Cα atoms in the model.

Cofactor binding

ThDP binds in a deep cleft at the interface between the two subunits and residues from both subunits contribute to cofactor binding. Enzyme bound ThDP has a more extended conformation than the crystal structure of isolated ThDP hydrochloride (Pletcher and Sax, 1972). Furthermore, the pyrimidine ring's conformation in relation to the thiazolium ring is different from that in the ThDP molecules that have been described (Pletcher and Sax, 1972; Shin *et al.*, 1979). ϕ_T, defined as the torsion angle C(5′)-C(3,5′)-(N3)-C(2) and ϕ_P, the angle N(3)-C(3,5′)-C(5′)-C(4′) have values 90° and −70° respectively. This conformation positions the 4′-NH_2 group close to the reactive C2 carbon atom of the

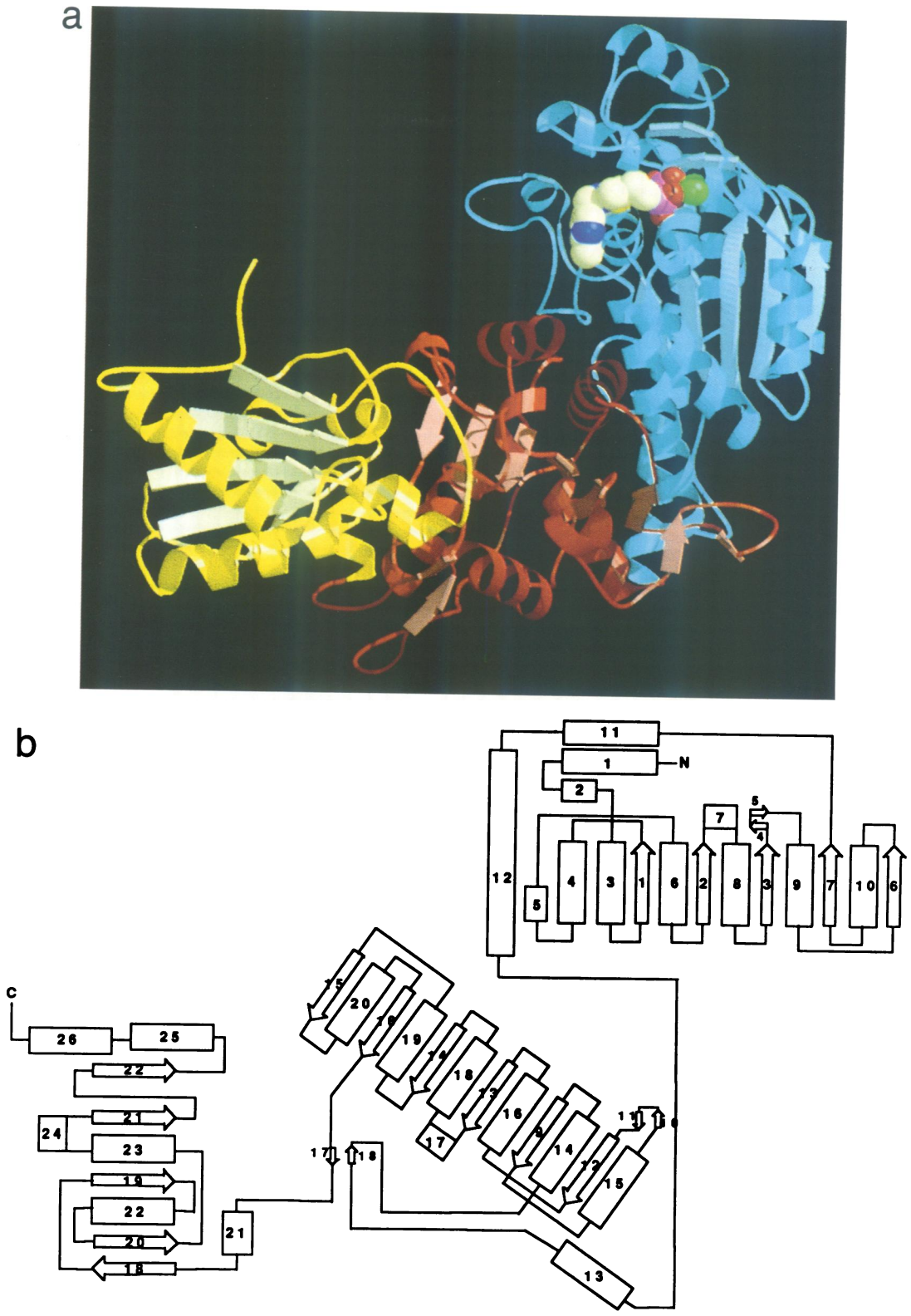

Fig. 2. (**a**) Schematic view of the structure of the transketolase subunit illustrating the domain organization. The three domains are colour coded differently: N-terminal domain, light blue; middle domain, red-brown; and C-terminal domain, yellow. The bound cofactor, ThDP, is shown as a CPK model. The Ca^{2+} ion is shown in green. Both this figure and Figure 3 were generated with the program MOLSCRIPT (Kraulis, 1991). (**b**) Topology diagram of the three domains, illustrating the fold of the transketolase subunit.

thiazolium ring while making this atom accessible for reaction.

The cofactor binds to the N-terminal domain at the carboxy end of the β-sheet, with the diphosphate group between strands 1 and 2. The diphosphate group of ThDP interacts with the protein in two ways, directly through hydrogen bonding and indirectly through co-ordination to a protein bound Ca^{2+} ion. The Ca^{2+} binding site is made up of three

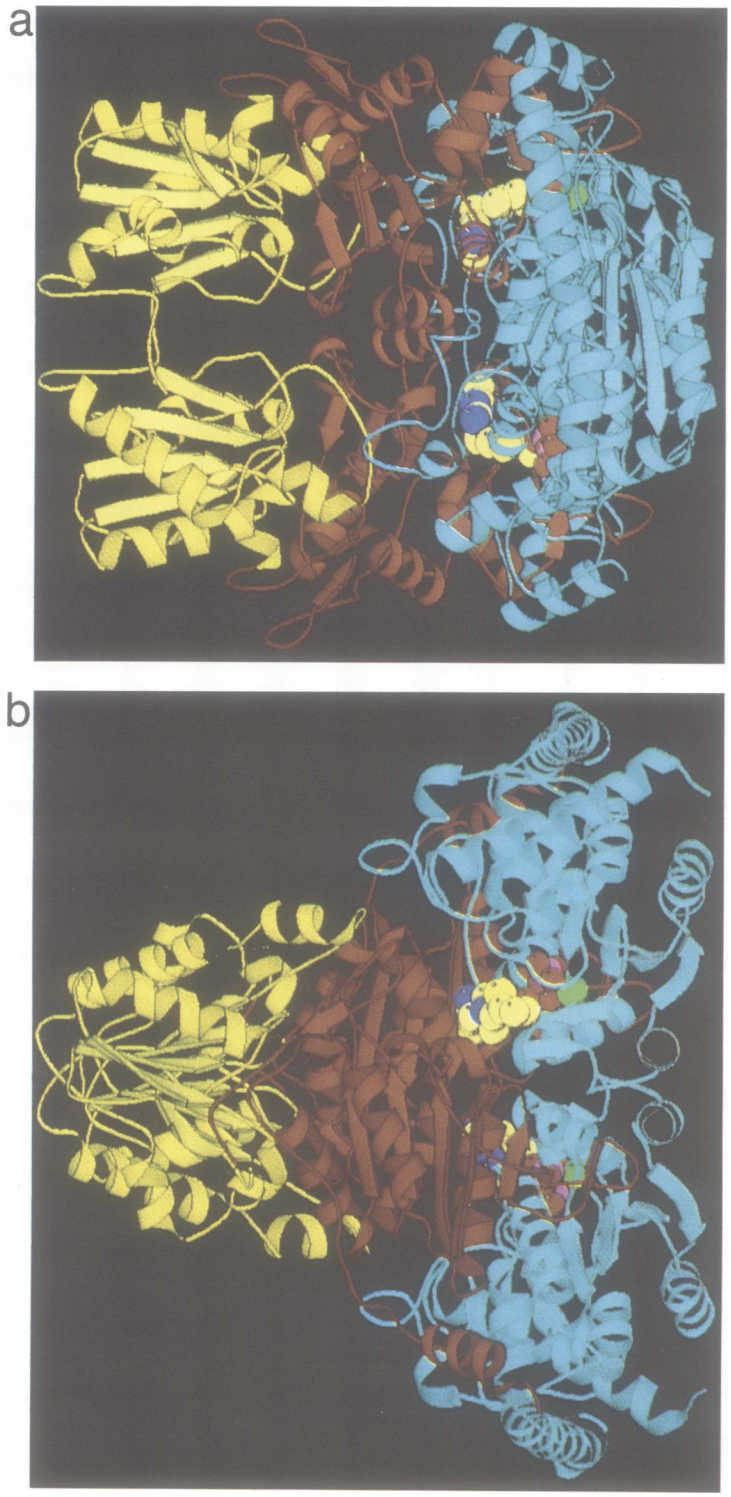

Fig. 3. Schematic view of the transketolase dimer. The bound cofactor and the metal ion are included. Colour coding is as in Figure 2a. The local twofold axis runs horizontally in the plane of the paper. (**a**) The dimer oriented as in Figure 2a. (**b**) The dimer rotated 90° about the local twofold axis.

protein ligands, the side chains of the conserved residues Asp157 and Asn187 and the main chain oxygen atom of Ile189 (Figure 4). Two oxygen atoms from the diphosphate are also ligands of the Ca^{2+} ion, giving pentameric coordination with square pyramidal geometry. Further interactions of the diphosphate with the protein are mediated through hydrogen bonds to two conserved histidine residues, His69 and His263. The terminal phosphate group is also close to the conserved residue Asp185. One of the oxygen atoms of the second phosphate group forms a hydrogen bond to the main chain nitrogen atom of Gly158 at the N-terminus of a short α-helix.

The remaining part of the cofactor, and the thiazolium and pyrimidine rings are bound in a cleft between the two subunits. This arrangement of the cofactor binding site in transketolase requires the dimer for proper, catalytically competent binding of ThDP. The thiazolium ring forms mainly hydrophobic interactions with the conserved residues

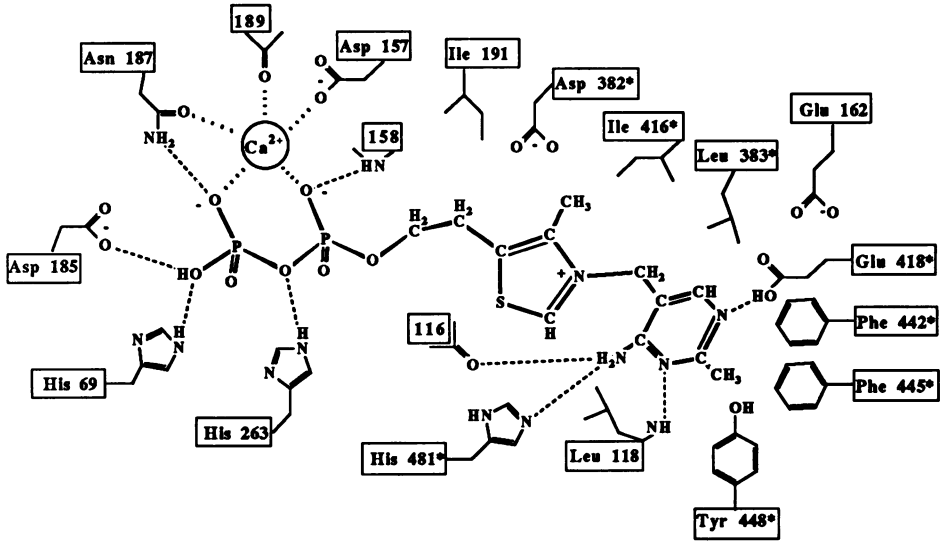

Fig. 4. Schematic diagram of the interactions of ThDP at the cofactor binding site of transketolase. All residues within 4 Å of the cofactor are included in the figure. Residues coming from the second subunit are indicated by an asterisk after the residue number. Possible hydrogen bonds are indicated by dashed lines.

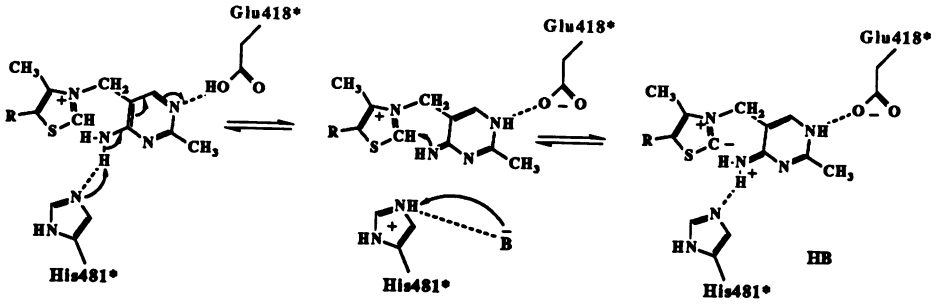

Fig. 5. Mechanism of proton abstraction at the C2 carbon atom of ThDP. B denotes an enzymic base or a water molecule.

Leu118 and Ile191 which pack against the ring. The C4 methyl group interacts with the side chains of the conserved Leu383* (the asterisk indicates a residue from the second subunit) and Ile416*. Close to the thiazolium ring, there is a side chain of Asp382*, which probably compensates for the positive charge of the thiazolium ring.

The pyrimidine ring is bound in a hydrophobic pocket built up by conserved residues Phe442*, Phe445* and Tyr448* from the second subunit. The pyrimidine ring of the cofactor is stacked with the ring system of Phe445*, whereas the methyl group points at right angles towards the plane of the Tyr448* ring. A number of hydrogen bonds participate in binding the pyrimidine ring and are responsible for the proper orientation of this part of the cofactor at the active site. The 4′-NH_2 group forms a hydrogen bond to the main chain oxygen of the conserved Gly116 in the first subunit and is also close to the His481* side chain. The N3′ nitrogen atom of the pyrimidine ring makes a hydrogen bond to the main chain nitrogen atom of Leu118. An important interaction is made by the N1′ of the pyrimidine ring which is hydrogen bonded to the side chain of Glu418*. This conserved side chain is in turn within a short distance from another conserved glutamic acid, Glu162. This implies that Glu418* is protonated, i.e. uncharged, since interaction of this side chain with the N1′ atom would not otherwise be possible. The interaction of the ring nitrogen with Glu418* is certainly of functional significance, since protonation of this nitrogen must influence the electronic properties of the 4′-NH_2 group which is in close spatial proximity to the C2 carbon atom of the thiazolium ring. The importance of this interaction is further substantiated by the fact that ThDP analogues in which the N1′ atom has been replaced by carbon are catalytically inactive (Meshalkina *et al.*, 1991). Replacement of the N3′ atom, however, does not interfere significantly with the coenzyme activity.

The cofactor is almost completely buried in its binding site. The C2 atom is the only atom which is accessible from solution through the active site cleft. All other cofactor atoms are not accessible to solvent. During turnover, the C2 atom forms a covalent adduct with the substrate, a mechanism common to all ThDP catalysed reactions.

Active site

The ThDP binding site is accessible from the solvent through a deep cleft between the two subunits. This cleft is lined with conserved residues, located on loop regions, which build up the active site. On one side of the thiazolium ring, in the vicinity of the C2 atom, is a cluster of conserved histidine residues, His30, His69, His103, His263 and His481*. Two of these residues are involved in binding the diphosphate group. The other histidines might function in proton transfer during catalysis and in the stabilization of the covalent intermediate between substrate and ThDP.

Towards the entrance to the active site cleft, ~12 Å away

from the thiazolium ring, we find two conserved arginine residues, Arg94 and Arg528*, which might be involved in binding the phosphate group of the substrate.

Several highly conserved loop regions are found as parts of this pocket. Amongst those loops is one of the longest stretches of conserved amino acids in the whole polypeptide chain (468*–483*), suggesting that this region is of functional importance. Two residues from this loop, Glu476* and Asp477* point into the active site cleft and might be part of the binding site for the donor and/or acceptor substrate.

Discussion

Based upon the comparison of amino acid sequences for a number of ThDP dependent enzymes, Hawkins *et al.* (1989) suggested a putative ThDP binding motif. This motif consists of the sequence -G-D-G- and a conserved asparagine residue, separated by 28 amino acids. This sequence motif was interpreted as being reminiscent of the fingerprint for the nucleotide binding fold. The three-dimensional structure of transketolase confirms that this fingerprint is involved in ThDP binding and reveals the structural reason for the conservation of these residues. The aspartic acid and the asparagine are ligands of the metal ion and the two glycine residues are located at the N-terminus of a short α-helix which is involved in the binding of one of the phosphate groups of ThDP. The structure involving these conserved amino acids is thus different from that of the Gly-X-Gly-X-X-Gly fingerprint found in nucleotide binding domains.

Upon binding of ThDP to apo-transketolase, a strong absorption in the 300–380 nm region of the CD spectrum has been observed (Kochetov *et al.*, 1970). This spectral change has been interpreted as being caused by charge transfer between the thiazolium ring of the cofactor and an enzymic tryptophan residue (Kochetov and Usmanov, 1970). The three-dimensional structure of holo-transketolase clearly shows that there is no tryptophan residue close enough to the cofactor for charge transfer to occur. However, the structure suggests that the strong absorption in the CD spectrum might be caused by a charge transfer complex between the pyrimidine ring of the cofactor and Phe445*.

A common initial step in thiamine catalysis is the deprotonation of the C2 atom of ThDP (Breslow, 1958). In the transketolase reaction, the carbanion formed then attacks the carbonyl group of the ketose substrate forming a covalent intermediate. In the structure of holo-transketolase, no enzymic base is close enough or has good enough geometry to abstract the C2 proton. We suggest that this proton is removed by the 4′-imino group of the cofactor as shown in Figure 5. Interaction of bound ThDP with the uncharged side chain of Glu418 leads to partial protonation of N1′ of the pyrimidine ring. Protonation of this ring nitrogen promotes a resonance form with a positively charged 4′-NH_2 group. One of these protons can now be abstracted by His481*, leading to a 4′-imino group at the pyrimidine ring. Model experiments by Jordan and coworkers (Jordan *et al.*, 1982) have shown that the protonation at N1′ is necessary for the exchange of NH_2 protons to occur, i.e. the 4′-NH_2 group can, under these conditions, function as an acid/base catalyst.

The protonated His481* side chain can transfer its proton to bulk solvent. The 4′-imino group of the pyrimidine ring is now a good candidate for the base that accepts the C2 proton. In the presence of donor substrate, the negatively charged C2 carbon atom can attack the carbonyl group of

Table I. Data collection and phasing statistics

Data collection Data set	Number of crystals	Resolution (Å)	Measured reflections	Unique reflections (% of total)	R_{merge}[a]
NATI1	2	2.9	71 017	23 796 (75)	0.078
NATI2	3	2.5	107 894	45 688 (91)	0.070
$K_2Hg(CN)_4$	1	2.9	48 999	25 236 (80)	0.038
METO1[b]	1	4.3	22 391	8692 (77)	0.078
METO2	1	2.9	39 657	16 531 (51)	0.059
UO_2Cl_2	1	4.4	21 537	7594 (71)	0.063
Ta_6Br_{12}	1	5.5	17 192	4195 (71)	0.067
Phasing statistics Derivative	Number of sites	R_{deriv}[c]	R_{cullis}[d]	Phasing power[e] (resolution, Å)	
$K_2Hg(CN)_4$[f]	1	0.157	0.74	1.41 (2.9)	
METO1[f]	5	0.171	0.73	1.14 (2.9)	
METO2	4	0.148	0.67	1.75 (4.3)	
UO_2Cl_2	5	0.134	0.68	1.44 (4.4)	
Ta_6Br_{12}	2	0.154	0.62	2.89 (5.5)	

[a] $R_{merge} = \Sigma\ \Sigma_i|I_i - \langle I\rangle| / \Sigma|\langle I\rangle|$ where I_i are the intensity measurements for a reflection and $\langle I\rangle$ is the mean value for this reflection.
[b] Methoxyethylmercuric chloride
[c] $R_{deriv} = \Sigma\ |F_{PH} - F_P| / \Sigma|F_P|$ where F_P is the structure factor amplitude of the derivative crystal and F_{PH} is that of the native.
[d] $R_{cullis} = \Sigma\ ||F_{PH}F_P| - |F_H(calc)|| / \Sigma\ |F_{PH} - F_P|$ where F_{PH} and F_P are defined as above and $F_H(calc)$ is the calculated heavy atom structure factor amplitude summed over centric reflections only.
[e] Phasing power: $= F(H)/E$, the r.m.s. heavy atom structure factor amplitudes divided by the lack of closure error.
[f] Anomalous dispersion data included in the refinement.

the ketose substrate. The protonated 4′-imino is then able to donate a proton to the keto-oxygen when the covalent adduct with substrate is formed, as has already been suggested by others (Schellenberger *et al.*, 1991). Assignment of residues involved in subsequent steps of the catalytic cycle must await determination of the structure of complexes of transketolase with donor and acceptor substrates, respectively.

Materials and methods

Crystallization, heavy metal derivatives and data collection

Commercially available *S.cerevisiae* transketolase (Sigma) was used without further purification. Crystals of holo-transketolase were obtained using 13–17% PEG 6000, 2 mM thiamine diphosphate and 5 mM $CaCl_2$ in 50 mM glycyl–glycine buffer, pH 7.9, as described previously (Schneider *et al.*, 1989). Holo-transketolase crystallizes in space group $P2_12_12_1$ (Konareva *et al.*, 1983; Schneider *et al.*, 1989) with cell dimensions a = 76.3 Å, b = 113.3 Å and c = 160.9 Å. These crystals contain one dimer in the asymmetrical unit.

Heavy metal derivatives were prepared by soaking crystals of the holoenzyme in the above solution with the addition of 5 mM heavy metal salt (in the case of the cluster compound Ta_6Br_{12}, only 1 mM) for 4–5 days. Native data set NATI1 and all derivative data sets were collected on a Nicolet multiwire area detector mounted on a Rigaku rotating anode. Reflections were measured in 0.1° oscillation frames and evaluated with the BUDDHA program (Blum *et al.*, 1987). Further processing and scaling were done with the program PROTEIN (Steigemann, 1974). Native data set NATI2 was collected on film at SRS Daresbury, UK. Films were processed using MOSFILM and the CCP4 program suite (Daresbury, UK). Details of data collection are given in Table I.

Phasing

Two heavy atom sites were located by manual inspection of the difference Patterson maps for the Ta_6Br_{12} and METO derivatives. The $K_2Hg(CN)_4$ derivative contains one major site, which could also be located easily. The remaining heavy atom sites were located by cross-phased difference Fourier maps. Refinement of the heavy metal parameters and calculation of phases was done using a program originally written by M.G.Rossmann. The two METO crystals were refined separately because they contained different number of sites with different occupancies. The mean figure of merit in the final run was 0.54 for all reflections to 2.9 Å resolution (Table I).

Non-crystallographic symmetry

Solvent flattening (Wang, 1985) was used to improve the initial multiple isomorphous replacement phases. The envelope of the molecule was defined from a skeletonized solvent flattened electron density map. The position of the local twofold symmetry axis was determined from the heavy metal positions. The program package of Bricogne (1976) was used for cyclic averaging and phase combination following a protocol described earlier (Schneider *et al.*, 1986). The final R-value was 0.170 and the correlation coefficient 0.91.

Model building

Skeletonized electron density maps ['bones' (Jones and Thirup, 1986)] were used to build the initial partial model. The atomic model was built with the graphics program O (Jones *et al.*, 1991). This model was refined with XPLOR (Brünger, 1989) and the calculated model phases were combined with multiple isomorphous replacement phases, followed by model building and refinement. This cyclic procedure gradually improved the electron density such that the chain could be traced and the amino acid side chains fitted to the electron density map. Simultaneously, the amino acid sequence derived from the nucleotide sequence of the transketolase gene from *S.cerevisiae* became available (M.Sundström, Y.Lindqvist, U.Hellman, G.Schneider and H.Ronne, unpublished) and could be fitted to the electron density map using the Slider option in O.

Refinement

The coordinates are presently being refined by simulated annealing using the program XPLOR. After the R-factor dropped below 0.24 at 2.5 Å resolution, the overall B-factor was replaced by restrained individual B-factors. The current model has a crystallographic R-factor of 0.215 in the resolution interval 8.0–2.5 Å with r.m.s. bond length deviations of 0.024 Å. The coordinates will be deposited with the Protein Data Bank, Brookhaven.

Acknowledgements

We thank Professor B.Bowien (Göttingen) and Dr G.Sprenger (Freiburg) for communicating unpublished results. We also thank the staff at the SRS Daresbury, UK for the use of synchrotron radiation. U.E. acknowledges an EMBO fellowship. This work was supported by a grant from the Swedish Natural Science Research Council and Magnus Bergvalls Stiftelse.

References

Blum,M., Metcalf,P., Harrison,S.C. and Wiley,D.C. (1987) *J. Appl. Crystallogr.*, **20**, 235–242.
Brändén,C.-I. (1980) *Q. Rev. Biophys.*, **13**, 317–338.
Breslow,R. (1958) *J. Am. Chem. Soc.*, **80**, 3719–3726.
Bricogne,G. (1976) *Acta Crystallogr. A*, **32**, 832–847.
Brünger,A.T. (1989) *Acta Crystallogr. A*, **45**, 50–61.
Cavalieri,S.W., Neet,K.E. and Sable,H.Z. (1975) *Arch. Biochem. Biophys.*, **171**, 527–532.
Chen,J.H., Gibson,J.L., McCue,L.A. and Tabita,F.R. (1991) *J. Biol. Chem.*, **266**, 20447–20452.
Egan,R.M. and Sable,H.Z. (1981) *J. Biol. Chem.*, **256**, 4877–4883.
Hawkins,C.F., Borges,A. and Perham,R.N. (1989) *FEBS Lett.*, **255**, 77–82.
Heinrich,P.C., Steffen,H., Janser,P. and Wiss,O. (1972) *Eur. J. Biochem.*, **30**, 533–541.
Janowicz,Z.A., Eckart,M.R., Drewke,C., Roggenkamp,R.O., Hollenberg,P., Maat,J., Ledeboer,A.M., Visser,C. and Verrips,C.T. (1985) *Nucleic Acids Res.*, **13**, 3043–3062.
Jones,T.A. and Thirup,S. (1986) *EMBO J.*, **5**, 819–822.
Jones.T.A., Zou,J.-Y. and Cowan,S.W. (1991) *Acta Crystallogr. A*, **47**, 110–119.
Jordan,F., Chen,G., Nishikowa,S. and Sundoro,W.B. (1982) *Ann. N.Y. Acad. Sci.*, **378**, 14–29.
Kluger,R. (1987) *Chem. Rev.*, **87**, 863–876.
Kochetov,G.A. and Usmanov,R.A. (1970) *Biochem. Biophys. Res. Commun.*, **41**, 1134–1140.
Kochetov,G.A., Usmanov,R.A. and Merzlov,V.P. (1970) *FEBS Lett.*, **9**, 265–266.
Konareva,N.V., Kuranova,J.P., Mikhailov,A.M., Usmanov,R.A. and Kochetov,G.A. (1983) *Biochem. Int.*, **6**, 799–803.
Kraulis,P. (1991) *J. Appl. Crystallogr.*, **24**, 946–950.
Meshalkina,L.E., Usmanov,R.A. and Kochetov,G.A. (1991) In Bisswanger,H. and Ullrich,J. (eds), *Biochemistry and Physiology of Thiamine Diphosphate Enzymes*. Verlag Chemie, Weinheim, pp. 343–352.
Pletcher,J. and Sax,M. (1972) *J. Am. Chem. Soc.*, **94**, 3998–4005.
Schellenberger,A., Neef,H., Golbik,R., Hübner,G. and König,S. (1991) In Bisswanger,H. and Ullrich,J. (eds), *Biochemistry and Physiology of Thiamine Diphosphate Enzymes*. Verlag Chemie, Weinheim, pp. 3–15.
Schneider,G., Lindqvist,Y., Brändén,C.-I. and Lorimer,G. (1986) *EMBO J.*, **5**, 3409–3415.
Schneider,G., Sundström,M. and Lindqvist,Y. (1989) *J. Biol. Chem.*, **264**, 21619–21620.
Shaw,P.J. and Muirhead,H. (1977) *J. Mol. Biol.*, **109**, 475–485.
Shin,W., Pletcher,J., Sax,M. and Blank,G. (1979) *J. Am. Chem. Soc.*, **101**, 2462–2469.
Steigemann,W. (1974) PhD thesis, Technische Universität München.
Wang,B.C. (1985) *Methods Enzymol.*, **115**, 90–112.

Received on February 7, 1992; revised on March 23, 1992